International Journal of Pharmaceutics 422 (2012) 160–169

Contents lists available at SciVerse ScienceDirect

International Journal of Pharmaceutics

journal homepage: www.elsevier.com/locate/ijpharm

Cocrystallization and amorphization induced by drug–excipient interaction improves the physical properties of acyclovir

Takaaki Masuda[a,b,*], Yasuo Yoshihashi[b], Etsuo Yonemochi[b], Kotaro Fujii[c], Hidehiro Uekusa[c], Katsuhide Terada[b]

[a] R&D Laboratories, POLA PHARMA INC., 560 Kashio-cho, Totsuka-ku, Yokohama, Kanagawa 244-0812, Japan
[b] Faculty of Pharmaceutical Sciences, Toho University, 2-2-1 Miyama, Funabashi, Chiba 274-8510, Japan
[c] Department of Chemistry and Materials Science, Tokyo Institute of Technology, 2 Ookayama, Meguro-ku, Tokyo 152-8551, Japan

ARTICLE INFO

Article history:
Received 6 August 2011
Received in revised form
17 September 2011
Accepted 23 October 2011
Available online 3 November 2011

Keywords:
Acyclovir
Drug–excipient interactions
Cocrystal
Amorphous
Dissolution rate
Transdermal absorption

ABSTRACT

Although acyclovir is one of the most important antiviral drugs used today, there are several problems with its physical properties. The aim of this study is to prepare cocrystals or amorphous complex of acyclovir using drug–excipient interactions to improve the physical properties of the drug, especially its dissolution rate and transdermal absorption. Screening for formation of cocrystals and the presence of amorphous acyclovir was conducted with various pharmaceutical excipinents, with the use of the solution-crystallization method and liquid-assisted cogrinding. The potential cocrystalline phase and the amorphized complex were characterized by PXRD, TG/DTA, IR, DSC and HPLC techniques. The screening indicated that acyclovir formed novel cocrystals with tartaric acid and was amorphized with citric acid. The acyclovir–tartaric acid cocrystal (ACV–TA cocrystal) structure was determined from synchrotron X-ray powder diffraction data. T_g of the amorphous acyclovir–citric acid compound (ACV–CA amorphous) was determined by DSC. The initial dissolution rate of the ACV–TA cocrystals was considerably faster than that of anhydrous acyclovir. *In vitro* skin permeation of ACV–CA amorphous from polyethylene glycol (PEG) ointment was remarkably higher than that of the crystalline acyclovir. We successfully improved the physical properties of acyclovir by the cocrystallization and amorphization techniques, using pharmaceutical excipients.

1. Introduction

A challenging tasks in the pharmaceutical industry is to discover ways to improve the physicochemical properties of active pharmaceutical ingredients (APIs). The solubility and dissolution rate affects the bioavailability of pharmaceutical solids (Brittain, 1999). The molecular weight, melting point and solubility of APIs affect the transdermal absorption (Guy and Hadgraft, 1988; Stott, 1998; Squillante et al., 1997). Therefore, in order to improve solubility and dissolution rate, formulation scientists often used various basic approaches such as formation of salts, polymorphic and amorphous forms, solid dispersions, and inclusion complexes (Berge et al., 1977; Kato et al., 1981; Serajuddin, 1999; Koizumi et al., 1987). Though salt formation is a widely implemented and convenient method of improving solubility, it suffers from some disadvantages, including a lack of ionizable groups on the APIs and the availability of only a limited number of nontoxic salt formers (Stahl and Wermuth, 2002). Furthermore, use of approaches such as creation of metastable crystal forms or amorphous forms of APIs may increase the likelihood of instability (Kaushal et al., 2004). Pharmaceutical cocrystals provide an alternative way to modify the physicochemical properties of APIs; besides salt formation, and polymorphic and amorphous forms, that all have limitations in their utility. For topically administered drugs, amorphous forms have advantages such as enhanced skin permeability (Inoue et al., 2005).

Cocrystals can be made of non-ionizable drugs, which cannot undergo salt formation. In addition, for ionizable drugs, the number of suitable cocrystal formers can exceed the number of suitable salt formers. For example, the ionizable drug piroxicam has more than 50 reported cocrystal formers (Childs and Hardcastle, 2007). With unique properties for each drug form, there is great potential to form highly soluble and stable pharmaceutical cocrystals. In addition, use of pharmaceutical excipients as cocrystal formers may lead to improved safety.

Acyclovir (Fig. 1a) is a synthetic purine nucleoside analogue with inhibitory activity against herpes simplex virus type 1 (HSV-1), 2 (HSV-2) and varicellar-zoster virus (VZV); it stops replication of

* Corresponding author at: R&D Laboratories, POLA PHARMA INC., 560 Kashio-cho, Totsuka-ku, Yokohama, Kanagawa 244-0812, Japan. Tel.: +81 45 826 7241; fax: +81 45 826 7259.
E-mail address: ta-masuda@pola-pharma.co.jp (T. Masuda).

0378-5173/$ – see front matter © 2011 Elsevier B.V. All rights reserved.
doi:10.1016/j.ijpharm.2011.10.046

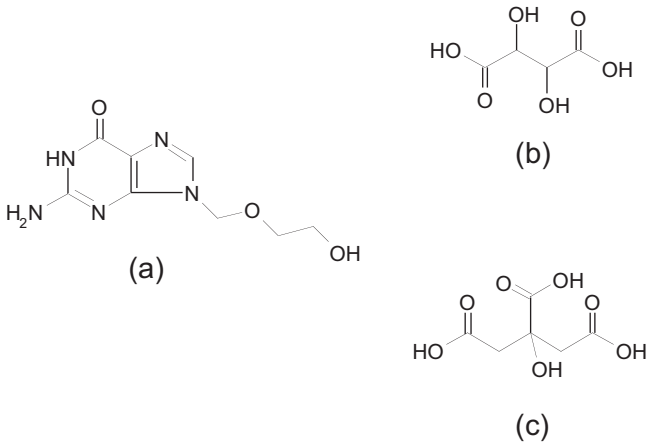

Fig. 1. Chemical structures of acyclovir (a), tartaric acid (b), and citric acid (c).

viral DNA due to its affinity for the enzyme thymidine kinase, which is encoded by HSV and VZV (Balfour, 1999).

Although acyclovir is one of the most important antiviral drugs, the drug has several problems due to its physical properties. For example, low bioavailability of acyclovir in solid pharmaceutical drugs is related to its poor solubility in aqueous media (Patel and Sawant, 2007). Acyclovir has absorption problems because of its low solubility and/or its saturable absorption mechanism that take place in the small intestine in a passive, variable, and incomplete manner. These factors therefore influence the oral bioavailability of acyclovir, which attains just 15–30% (Luengo et al., 2002). Acyclovir exists in a hydrated form with a ratio of acyclovir to water molecules in the crystal structure of 3:2 (Kristl et al., 1996). Acyclovir also exists in two anhydrated crystalline forms (Sohn and Kim, 2008). Recently, it was discovered that acyclovir exists in another hydrated form and that the ratio between acyclovir and water molecules in this crystal structure is 1:2 (Lutker et al., 2011). However, the hydrated and anhydrated forms were poorly soluble in aqueous media (Kristl et al., 1996). To improve the solubility of acyclovir, the preparation of a solid dispersion, an inclusion complex and a microemulsion of acyclovir were attempted (Patel and Sawant, 2007; Sachan et al., 2010; Rossel et al., 2000). In contrast, although several reports show that the solubility of several drugs is improved by cocrystallization, cocrystals of acyclovir have not been described. The first aim of this study was thus to improve the physical properties of the poorly soluble drug acyclovir by cocrystallization with the use of drug–excipient interactions.

Acyclovir also has problems in respect of transdermal absorption. Topically administered acyclovir in polyethylene glycol (PEG) has proved disappointing in the therapy of recurrent HSV infections in immunocompetent patients (Corey et al., 1982; Luby et al., 1984; Reichman et al., 1983; Spruance et al., 1982, 1984). Investigators have speculated from this experience that the failure of topical acyclovir therapy is due to the inability of acyclovir to penetrate the stratum corneum barrier layer of the skin (Luby et al., 1984; Spruance et al., 1984; Whitley et al., 1984). To investigate the poor drug delivery that results from this formulation, *in vitro* skin permeation of topical acyclovir in ointment was evaluated (Freeman et al., 1986). These researchers indicated that the use of PEG as a topical drug delivery vehicle was associated with poor drug delivery. In the other words, the poor clinical results seen with topical use of acyclovir ointment may be due to in part to retarded drug delivery from this formulation. The effect of PEG on skin penetration has been postulated to be due to a drug-vehicle interaction that results in a lower thermodynamic activity of the drug (Davis et al., 1981; Hadgraft, 1983; Higuchi, 1960). According to this hypothesis, increasing the thermodynamic activity of the drug in PEG ointment may lead to improvement of transdermal absorption. Several techniques have been developed to enhance transdermal absorption of drugs. In general, they can be classified into two types (Benson, 2005). The first type modifies the barrier properties of skin by chemical enhancers or physical methods such as iontophoresis or sonophoresis. However, significant skin toxicity sometimes limits the possible use of these techniques for clinical applications. The second type of technique utilizes modification of the thermodynamic activity of the drug molecules in vehicles. This does not require physicochemical alteration of the skin barrier, and therefore will be safer than former approach. Several methods have been reported to enhance the thermodynamic activity of drugs. A method that used supersaturation generated by an amorphous drug was reported to enhance the thermodynamic activity of the drug (Szeman et al., 1987). In a supersaturated system, the drug molecules are present in amounts that exceed the solubility of the drug, as they are dispersed in a vehicle, resulting in temporarily high thermodynamic activity, thereby leading to high skin permeability. Therefore, the second aim of this study was to improve transdermal absorption of acyclovir by enhancing the thermodynamic activity of the drug in PEG ointment through amorphization of the drug. The application of acyclovir amorphous to enhance transdermal absorption of this drug has not been reported.

In the present study, we found that novel cocrystals of acyclovir are formed by interactions between the drug and the pharmaceutical excipient L-tartaric acid (Fig. 1b), and that a novel amorphous form of the drug results from interactions between the drug and the pharmaceutical excipient anhydrous citric acid (Fig. 1c). This paper describes the pharmaceutical characterization of the acyclovir–tartaric acid cocrystal (ACV–TA cocrystal) and acyclovir–citric acid amorphous (ACV–CA amorphous). The physical state of the ACV–TA cocrystals was characterized by PXRD, TG–DTA, IR and HPLC, and that of ACV–CA amorphous was characterized by PXRD, DSC and HPLC. The ACV–TA cocrystal structure was determined from synchrotron X-ray powder diffraction data. Pharmaceutical characterization of the ACV–TA cocrystals included dissolution studies, and that of ACV–CA amorphous included *in vitro* skin permeation studies.

2. Materials and methods

2.1. Materials

Acyclovir (the two-thirds hydrated form) was purchased from Zhejiang Zhebei Pharmaceutical Co., Ltd. (Zhejiang, China). Other agents including L-tartaric acid and anhydrous citric acid were purchased from Wako Pure Chemical Industries Ltd. (Osaka, Japan).

2.2. Preparation of acyclovir polymorph forms

Acyclovir anhydrous form 1 was obtained by recrystallization after dissolving the two-thirds hydrated form in *N*,*N*-dimethylformamide using acetonitrile as a poor solvent. The anhydrous form 2 was obtained by drying the two-thirds hydrated form at 180 °C for 1 h. The dihydrated form was obtained by recrystallization after dissolving the anhydrous form 2 in water.

2.3. Screening for acyclovir cocrystals and amorphous forms

Acyclovir anhydrous form 2 was the drug used. Several cocrystal formers in suitable molar ratio were selected from a range of dicarboxylic acids, higher fatty acids, amino acids, urea, nicotinamide and saccharin. The solution method (cooling or slow evaporation of the solvent) and liquid-assisted (solvent-drop) grinding (Friščić et al., 2006) were employed in screening for cocrystals and amorphous forms. A number of solvents, including water,

methanol, ethanol, acetonitrile, chloroform, *n*-hexane, cyclohexane, *N*,*N*-dimethylformamide and acetic acid, were used. Although several potential cocrystals were obtained, the ACV–TA cocrystal was the only cocrystal that was obtained reproducibly. The amorphized complex of acyclovir and citric acid was obtained by the solution method using *N*,*N*-dimethylformamide.

2.4. Cocrystallization of acyclovir–tartaric acid

A 1:1 mixture of acyclovir anhydrous form 2 (225.21 mg, 1 mmol) and L-tartaric acid (150.09 mg, 1 mmol) was dissolved in 30 mL of glacial acetic acid (99.7%) under constant stirring at 60 °C. The solution was filtered and cooled at room temperature. The resulting crystals were filtered and dried in a desiccator over silica gels at room temperature. ACV–TA cocrystals were also obtained by the solvent-drop grinding method using *N*,*N*-dimethylformamide. A 1:1 mixture of acyclovir anhydrous form 2 (225.21 mg, 1 mmol) and L-tartaric acid (150.09 mg, 1 mmol) was ground manually in an agate mortar at room temperature for 5 min together with the addition of a few drops of *N*,*N*-dimethylformamide.

2.5. Amorphization of acyclovir–citric acid

Acyclovir anhydrous form 2 (225.21 mg, 1 mmol) and an excessive amount of anhydrous citric acid (1921.24 mg, 10 mmol) were suspended in 30 mL of *N*,*N*-dimethylformamide under constant stirring at 60 °C. The hot suspension was rapidly filtered to remove all nuclei, and then the solvent was then slowly evaporated at room temperature. The coprecipitates were dried in a desiccator over silica gels at room temperature.

2.6. Preparation of physical mixtures

A physical mixture of acyclovir and tartaric acid (ACV–TA-PM) was prepared by mixing acyclovir anhydrous form 2 and L-tartaric acid (ratio of the drug and pharmaceutical excipient was 1:1) using a vortex mixer (Labo-Mixer NS-8: Pasolina Co., Ltd., Tokyo, Japan) for 10 min at a shaking speed of 3000 rpm. A physical mixture of acyclovir and citiric acid (ACV–CA-PM) was prepared by mixing the anhydrous form 2 and anhydrous citric acid (ratio of the drug and pharmaceutical excipient was 1:2) using the vortex mixer for 10 min at above-mentioned condition.

2.7. Solid analysis

2.7.1. Powder X-ray diffractometry (PXRD)

The PXRD patterns of all samples were collected in reflectance mode using a Bruker D8 Discover with a GADDS CS diffractometer (Bruker AXS GMBH, Karlsruhe, Germany) using Cu Kα radiation with a graphite monochromator and a 0.3-mm single pinhole collimator. The tube voltage and amperage were set to 40 kV and 40 mA, respectively. The diffractometer was equipped with an *XYZ* sample stage and a Hi-STAR area detector located 25 cm ($2\theta = 5–25°$) from the sample. The acquisition time was 180 s per frame.

2.7.2. Thermogravimetric/differential thermal analysis (TG/DTA)

TG/DTA was conducted using a Thermo Plus TG-8120 (Rigaku Corporation, Tokyo, Japan). All measurements were carried out in open aluminum pans, heated from 25 °C to 300 °C at a heating rate of 10 °C/min under a nitrogen purge. All samples were accurately weighed (1–7 mg).

2.7.3. IR spectroscopy

FT/IR-4100 (JASCO Corporation, Tokyo, Japan) was used in attenuated total reflectance (ATR) mode for collecting the IR spectra of the samples. The spectra were collected over the range of 4000–1000 cm^{-1} in 32 scans, with a resolution of 4 cm^{-1} for each sample.

2.7.4. Differential scanning calorimetry (DSC)

A Perkin Elmer DSC-7 (PerkinElmer, Inc., MA, USA) was used to determine the glass transition temperature (T_g) of the amorphized complex. The sample (3 mg) was crimped in a non-hermetic aluminum pan and scanned at a heating rate of 10 °C/min in the range of −40 to 100 °C under a nitrogen purge.

2.7.5. Drug/excipient composition analysis

Drug content in the cocrystals or amorphous form was assayed by HPLC to determine drug/excipient composition. Excipient content was calculated by subtracting the drug content from total weight.

2.7.6. Synchrotron X-ray powder diffraction

The synchrotron X-ray powder diffraction data of the ACV–TA cocrystals was collected using 1.19601 Å wavelength synchrotron radiation at 300 K with multiple-detector system on beam-line BL-4B2 at the Photon Factory in Tsukuba, Japan. The crystal structure was solved by the simulated annealing method (Kirkpatrick et al., 1983) using the program DASH (David et al., 2006). In this calculation, the measured powder pattern was subjected to a Pawley refinement (Pawley, 1981) in space group $P2_1$ in order to extract correlated integrated intensities from the pattern. The structure that give the best fit to the data was validated by Rietveld refinement of the fractional coordinates obtained at the end of the simulated annealing run. Rietveld refinement was performed using the program GSAS (Larson and Von Dreele, 2004).

2.8. Solubility and dissolution studies of the cocrystals

To determine the saturated solubility of acyclovir, ACV–TA-PM and ACV–TA cocrystals in distilled water, phosphate buffer pH 6.8 and ethanol, about 500 mg of each sample was added to 10 mL of each solvent, and the resulting slurry was stirred at 500 rpm on a magnetic stirrer at 25 °C for 24 h. An aliquot of the slurry was filtered through a 0.45 μm syringe filter. A 1 mL sample of the filtered aliquot was diluted to 100 mL with distilled water. The diluted sample was then assayed by HPLC to determine the concentration of acyclovir.

The dissolution test was conducted using a dissolution apparatus (TDS-30, Toyama Sangyo Co., Ltd., Osaka, Japan) to determine the initial dissolution rate of the cocrystals. For the dissolution test, about 100 mg of each of the samples (acyclovir polymorphic forms, ACV–TA-PM and ACV–TA cocrystals) was compressed into a 0.2 cm^2 disk by a press at a pressure of 1 ton/g for 1 min using a die with a hole 0.45 cm in diameter. The disk exposed a smooth surface on one side of the die; the other side of the die was sealed. In each experiment, three 1000 mL dissolution test vessels containing 900 mL of phosphate buffer at pH 6.8 were equilibrated at 37.0 °C with a paddle speed of 50 rpm. Experiments were run in triplicate. For all samples, the initial dissolution rate was calculated using data from 0 to 5 min. Drug concentrations were assayed by HPLC.

2.9. Preparation of PEG ointments containing either 5% acyclovir or ACV–CA-PM or ACV–CA amorphous

A PEG ointment of ACV–CA amorphous was prepared to evaluate the enhancement of the transdermal absorption by amorphization of the drug. The PEG ointment base was made in PEG 400 and PEG 4000. PEG 400 and PEG 4000 were purchased from NOF CORPORATION (Tokyo, Japan). Formulations containing either 5% acyclovir or ACV–CA-PM or ACV–CA amorphous in PEG were made by melting the ointment base at 50 °C, adding 5% (w/w) of the drug or the

physical mixture or the amorphous form, and completely mixing at room temperature until the formulation reverted to the semisolid characteristics of the base.

2.10. Solubility of acyclovir in PEG ointment base

The solubility of a drug in an ointment base is an important factor that determines the efficacy of the formulation. However, it is difficult to measure the solubility of a drug in an ointment base. One reported method is to measure the drug concentration in the bleeding liquid which leaks out from the ointment base (Kobayashi and Saitoh, 1998).

In this study, PEG 400 and PEG 4000 were used as the ointment base. PEG 400 is a viscous 'liquid'; on the other hand, PEG 4000 is a flaky solid. However, it is difficult to separate PEG 400 from the ointment base formed by the mixture of PEG 400 and PEG 4000. Thus, the solubility of two forms of acyclovir (crystalline and amorphous) in PEG ointment base was estimated using the saturated solubility of the drug in PEG 400 as the liquid ingredient in the ointment base.

To determine the saturated solubility of acyclovir, ACV–CA-PM and ACV–CA amorphous in PEG 400, about 50 mg of each of the samples was added to 5 mL of PEG 400, and the resulting slurry was stirred at 500 rpm on a magnetic stirrer at 25 °C for 24 h. An aliquot of the slurry was filtered through a 0.45 μm syringe filter. A 1 mL sample of the filtered aliquot was diluted to 10 mL with distilled water. The diluted sample was then assayed by HPLC to determine the concentration of acyclovir.

2.11. In vitro release of acyclovir from PEG ointment

Three replicate experiments using Franz-type diffusion cells (Hanson Research, Inc., CA, USA) were carried out to compare the *in vitro* release of two forms of acyclovir (crystalline and amorphous) from PEG ointment. Approximately 300 mg of each of the formulations (PEG ointments containing either 5% acyclovir or ACV–CA-PM or ACV–CA amorphous) was used. Nylon membranes (HNWP02500, 170 μm thickness) 0.45 μm pore size (Nihon Millipore K.K., Tokyo, Japan) were used. The temperature of the diffusion cell system was maintained by a water jacket kept at 32 °C, and 7 mL of release medium (phosphate buffer pH 6.8) kept at 32 °C was placed in the receptor chamber. During the experiments, the release medium was continuously stirred with a magnetic stirrer at 500 rpm. Aliquots of 1 mL of the release medium were withdrawn from the receptor chamber at predetermined times and replaced with the same volume of fresh buffer kept at 32 °C. The release experiments lasted for 360 min. The concentrations of acyclovir in the collected release medium were determined by HPLC to calculate the cumulative amount of released acyclovir. The cumulative amount of released acyclovir was plotted against the square root of time to obtain the release rate of acyclovir from PEG ointment. The release rate of acyclovir from the PEG ointment containing ACV–CA amorphous was compared with that from the PEG ointment containing either the crystalline acyclovir or the ACV–CA-PM to evaluate the enhancing effect of amorphization.

2.12. In vitro skin permeation experiments

In order to evaluate the enhancing effect of amorphization of the drug, the *in vitro* skin permeability of the PEG ointment containing amorphous acyclovir (ACV–CA amorphous) was compared with that of the PEG ointment containing either the crystalline acyclovir or the ACV–CA-PM. Laboskin (Hoshino Laboratory Animals, Inc., Ibaraki, Japan) was used for skin samples. Laboskin is a skin sample excised from the back of male hairless mice (Hos: HR-1), 7 weeks old, and cryopreserved at −20 °C. Immediately before the experiments, the frozen skin samples were slowly thawed at room temperature, and cut into pieces to mount on a Franz-type diffusion cell. The diffusion cell was the same as that used in the release experiments. The receptor fluid was also the same as that used in the release experiments (i.e., phosphate buffer, pH 6.8). The temperature of the diffusion cell system was maintained by a water jacket kept at 37 °C. The permeation was initiated by applying approximately 200 mg of the PEG ointment to the skin. One mL aliquots of the receptor fluid were then withdrawn from the receptor chamber at predetermined times and replaced with the same volume of fresh buffer kept at 37 °C. The permeation experiments lasted for 26 h. During the experiments, the receptor fluid was stirred continuously with a magnetic stirrer at 500 rpm. From the concentrations of acyclovir in the collected receptor fluid measured by HPLC, the cumulative amount of acyclovir permeated per unit area of the skin was calculated. For each PEG ointment, the skin permeation experiments were conducted in triplicate. The cumulative amount of permeated acyclovir was plotted against the sampling time to obtain the permeation profile, and the skin permeation flux was calculated from the slope of the linear portion of the permeation profile. The flux of the PEG ointment containing ACV–CA amorphous was compared with that of the PEG ointment containing either the crystalline acyclovir or the ACV–CA-PM to evaluate the enhancing effect of amorphization.

2.13. HPLC assay

In this study, a high performance liquid chromatography system (HPLC; Agilent 1100, Agilent Technologies, Inc., CA, USA) was used to assay the concentration of acyclovir. The HPLC system was equipped with a C18 column (Inertsil ODS-3 5 μm 4.6 mm × 250 mm, GL Sciences Inc., Tokyo, Japan). The mobile phase consisting of water/acetonitrile/acetic acid (959:40:1) was injected onto the column. UV detection took place at 254 nm.

3. Results and discussion

3.1. Cocrystal and amorphous screening and solid analysis

The results of the screening are summarized in Table 1.

The formation of cocrystals was confirmed by the screening of the combination of acyclovir and tartaric acid. The solvents that resulted in the novel cocrystals were *N*,*N*-dimethylformamide and acetic acid. In addition, an amorphized complex was obtained by the combination of acyclovir and citric acid. Acyclovir and citric acid were amorphized by the effect of *N*,*N*-dimethylformamide. The PXRD patterns for acyclovir (anhydrous form 1 and form 2, two-thirds hydrated form and dihydrated form), tartaric acid, ACV–TA cocrystals and ACV–CA amorphous are shown in Fig. 2.

The unique PXRD pattern of the ACV–TA cocrystals was distinguishable from acyclovir and tartaric acid. This result indicates the formation of a new crystal phase. No peaks were observed in ACV–CA amorphous except for a harrow-like pattern at 2θ degree between 5° and 25°, thus confirming its amorphous state.

The physical properties of the ACV–TA cocrysta1 were investigated in more detail by TG/DTA and IR techniques. As shown in Fig. 3, the TG/DTA curve of the ACV–TA cocrystals was also distinguishable from acyclovir and tartaric acid, and suggested that it was a nonsolvate crystal. The DTA thermogram for ACV–TA cocrystals showed a single endothermic transition attributed to the melting transition. The thermal behavior of the cocrystals was distinct, with a different melting transition from that seen with either of the individual components; this suggests the formation of a new phase. The single endothermic transition and TG curve for the cocrystals indicates that the absence of any unbound or absorbed solvent and also demonstrates the stability of the phase until the melting point.

Table 1
Summary of cocrystal and amorphous screening.

Cocrystal formers	Solvents								
	Distilled water	Methanol	Ethanol	Acetonitrile	Chloroform	*n*-Hexane	Cyclohexane	DMF	Acetic acid
Citric acid	NC	ACV	ACV	ACV	M	M	M	Amorphous	ACV
L-Tartaric acid	ACV	NC	NC	ACV	M	M	M	Cocrystal	Cocrystal
DL-Malic acid	ACV	ACV	ACV	ACV	M	M	M	NC	ACV
Stearic acid	–	M	–	–	–	–	–	–	–
Palmitic acid	–	M	–	–	–	–	–	–	–
Docosanoic acid	–	M	–	–	–	–	–	–	–
Lauric acid	–	M	–	–	–	–	–	–	–
Glycine	ACV	ACV	ACV	M	–	–	–	–	–
DL-Alanine	ACV	M	M	M	–	–	–	–	–
L-Aspartic acid	ACV	M	M	M	–	–	–	–	–
L-Arginine	ACV	M	M	M	–	–	–	–	–
Urea	ACV	ACV	–	–	M	M	M	Cocrystal[a]	–
Nicotinamide	ACV	ACV	ACV	ACV	–	–	–	ACV	–
Saccharin	Cocrystal[a]	ACV	–	ACV	–	–	–	–	–

Endash (–): test not conducted, NC: not crystallized (paste state), ACV: crystallization of acyclovir hydrate or anhydrous, M: mixture of drug and cocrystal former.
[a] The cocrystals were not obtained again despite several attempts under similar conditions.

The IR spectra for acyclovir (anhydrous form 1 and form 2), tartaric acid and the ACV–TA cocrystals are represented in Fig. 4.

The IR spectrum of acyclovir anhydrous had two peaks in the region of 3500–3300 cm^{-1}, corresponding to primary and secondary amines, respectively, and the 1600 cm^{-1} region was represented by a band corresponding to the amide group (Fig. 4a and b) (Barboza et al., 2009). The spectrum of tartaric acid had two peaks at 3405 and 3336 cm^{-1} corresponding to a O–H group, and the region of 1737 cm^{-1} showed a band corresponding to C=O stretch (Fig. 4c) (Kozhevina et al., 1980). The N–H stretching frequency of the primary amine group of acyclovir and the O–H stretching frequency of the carboxyl group of tartaric acid were observed at 3476 and 3328 cm^{-1}, respectively, in ACV–TA cocrystals (Fig. 4d). This suggests that acyclovir and tartaric acid molecules are present in the new phase. The increase in the N–H stretching frequency from 3432 cm^{-1} in the anhydrous form of acyclovir to 3476 cm^{-1} in the ACV–TA cocrystals implies that the primary amine group is participating in a weak hydrogen bond. In addition, the decrease in the N–H bending frequency (amide) from 1599 cm^{-1} in the anhydrous form of acyclovir to 1592 cm^{-1} in ACV–TA cocrystals implies that the N–H group of an amide is participating in a strong hydrogen bond. Subsequently, the decrease in the O–H stretching frequency from 3336 cm^{-1} in tartaric acid to 3328 cm^{-1} in ACV–TA cocrystals suggests that the carboxyl group is participating in a strong hydrogen bond. A bathochromic shift in the C=O stretching frequency in tartaric acid from 1737 cm^{-1} to 1710 cm^{-1} further explains the formation of the ACV–TA cocrystals.

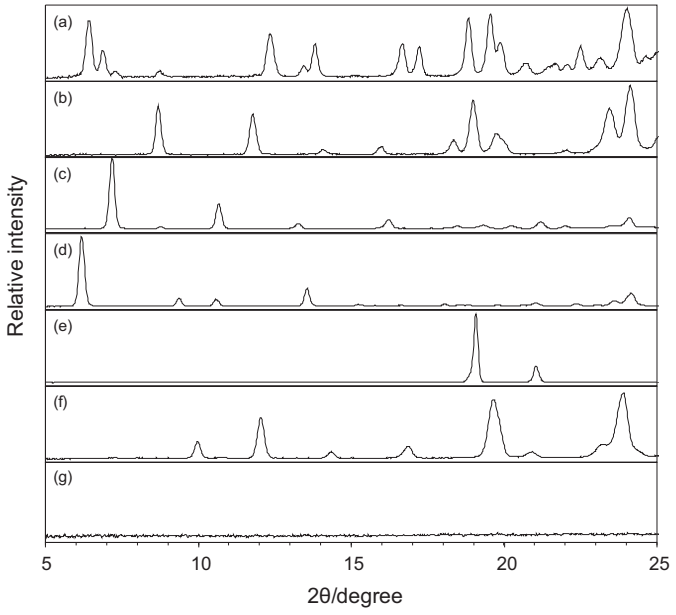

Fig. 2. PXRD patterns of acyclovir (anhydrous form 1 (a), anhydrous form 2 (b), two-thirds hydrate (c), dihydrate (d)), tartaric acid (e), ACV–TA cocrystals (f), and ACV–CA amorphous (g).

The IR spectra for acyclovir (anhydrous form 1 and form 2), citric acid, the ACV–CA-PM and the ACV–CA amorphous are represented in Fig. 5.

The IR spectrum of citric acid had characteristic peaks of crystalline anhydrous citric acid at 3495 and 3287 cm^{-1} corresponding to a O–H group (Fig. 5c) (Rao and Narayanaswamy, 1970). In the intermediate frequency region, we detected the C=O stretching of anhydrous citric acid at 1698 cm^{-1}. Dimerisation usually occurs in the C=O stretching in the range 1690–1720 cm^{-1}. The peak at 1746 cm^{-1} was connected to the O–H stretching lowered due to hydrogen bonding (Rao and Narayanaswamy, 1970). No shifts were observed in the peaks of the IR spectrum for the ACV–CA-PM (Fig. 5d). This indicates that the physical mixture spectrum was only the summation of acyclovir and citric acid spectrum, and reflected that there were no interaction between acyclovir and citric acid in the physical mixture. In the ACV–CA amorphous, the peak at 3495 cm^{-1} corresponding to a O–H group of citric acid vanished and the N–H stretching frequency from 3396 cm^{-1} in the anhydrous form of acyclovir shifted to 3402 cm^{-1} (Fig. 5e). In addition, the O–H stretching frequency at 1746 cm^{-1} in citric acid vanished or merged with the C=O stretching band. These results indicate possibility of hydrogen bonding interaction between acyclovir and citric acid in the ACV–CA amorphous.

Fig. 6 shows the DSC curve of ACV–CA amorphous.

It demonstrates one glass transition for the complex, indicating that acyclovir and citric acid are miscible in the amorphous state. Citric acid has a glass transition temperature (T_g) of 11 °C (Lu and Zografi, 1997). On the other hand, the value of T_g of acyclovir has not been reported. The value of T_g of ACV–CA amorphous was 68 °C, indicating that the binary amorphous has a higher T_g than ambient temperature. In other words, the binary amorphous seemed to be stable at ambient temperature.

Acyclovir content in the ACV–TA cocrystals and ACV–CA amorphous was determined by HPLC. The percentage of the drug in the cocrystals was 59.44 ± 0.81 (%). The calculated content of the excipient, therefore, was 40.56 ± 0.81 (%). The molar ratio of acyclovir and tartaric acid was determined to be 1:1 since the theoretical percentage of the two components are 60.01% and 39.99%. On the

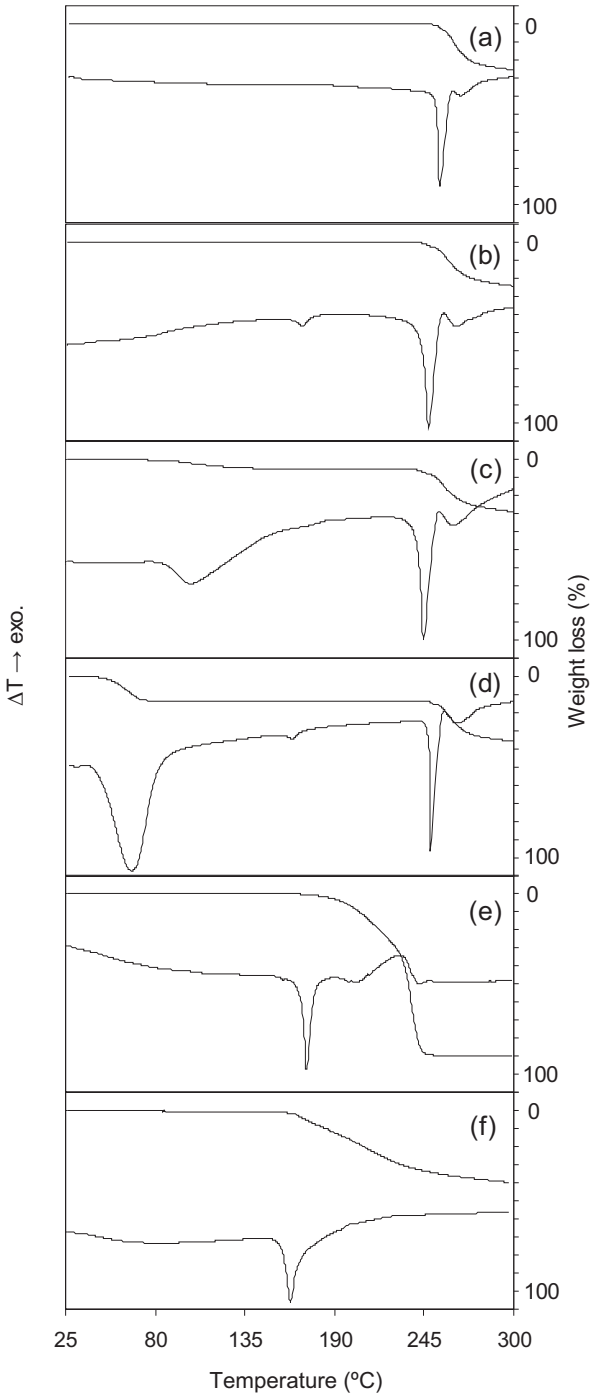

Fig. 3. TG/DTA curves of acyclovir (anhydrous form 1 (a), anhydrous form 2 (b), two-thirds hydrate (c), dihydrate (d)), tartaric acid (e), and ACV–TA cocrystals (f).

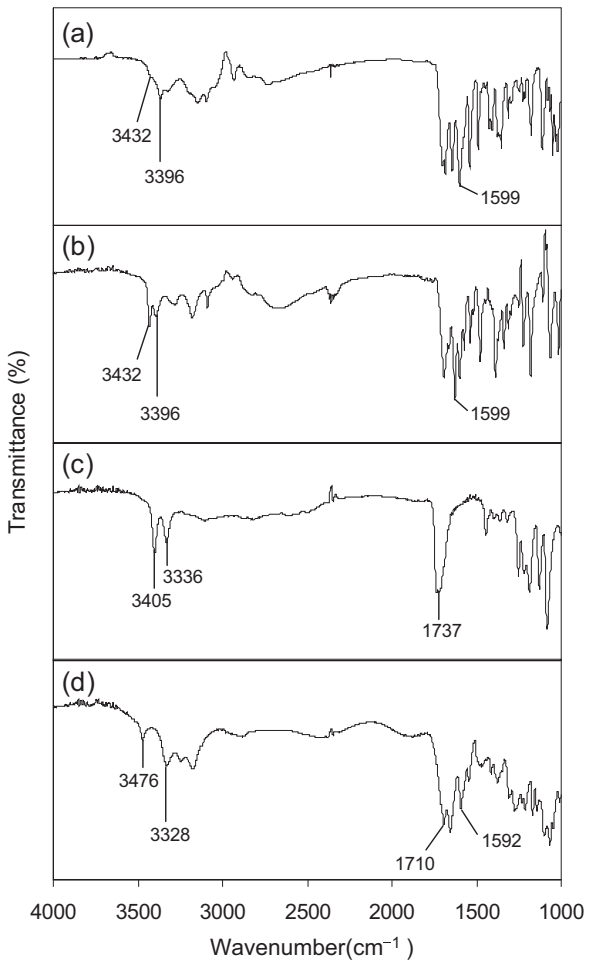

Fig. 4. IR spectra for acyclovir (anhydrous form 1 (a), anhydrous form 2 (b)), tartaric acid (c), and ACV–TA cocrystals (d).

Table 2
Crystallographic data and refinement parameter of ACV–TA cocrystal.

Empirical formula	$C_{12}H_{17}N_5O_9$
Formula weight	375.3
Crystal system	Monoclinic
Space group	$P2_1$
a (Å)	11.7087 (6)
b (Å)	14.9600 (8)
c (Å)	4.60203 (20)
α (°)	90.0000
β (°)	100.6006 (28)
γ (°)	90.0000
Volume (Å^3)	792.344
Z	2
D_{calc} (g/cm^3)	1.573
No. of reflections collected	7598
No. of unique reflections	1095
Rp	0.070
Rwp	0.107
R_F^2	0.124

other hand, the percentage of acyclovir and citric acid in the amorphous were 37.26 ± 0.73 (%) and 62.74 ± 0.73 (%), respectively. The molar ratio of acyclovir and citric acid was determined to be 1:2 since the theoretical percentage of the two components are 36.95% and 63.05%.

The crystal structure of the ACV–TA cocrystal was confirmed by synchrotron X-ray powder diffraction analysis. The crystallographic data of the cocrystal are summarized in Table 2 and the crystal structure is shown in Fig. 7.

In the ACV–TA cocrystal, the primary amine group and the secondary and tertiary amine groups in the purine ring of acyclovir formed hydrogen bonds with the hydroxyl group and the two carbonyl groups of tartaric acid. The molar ratio of acyclovir and tartaric acid in the ACV–TA cocrystal was 1:1 (Fig. 7). This molar ratio was also consistent with the result of HPLC assay.

3.2. Dissolution studies of the cocrystals

The saturated solubility of the ACV–TA cocrystals, acyclovir anhydrous form 2 and ACV–TA-PM in distilled water, phosphate buffer pH 6.8 and ethanol was determined by HPLC to compare the

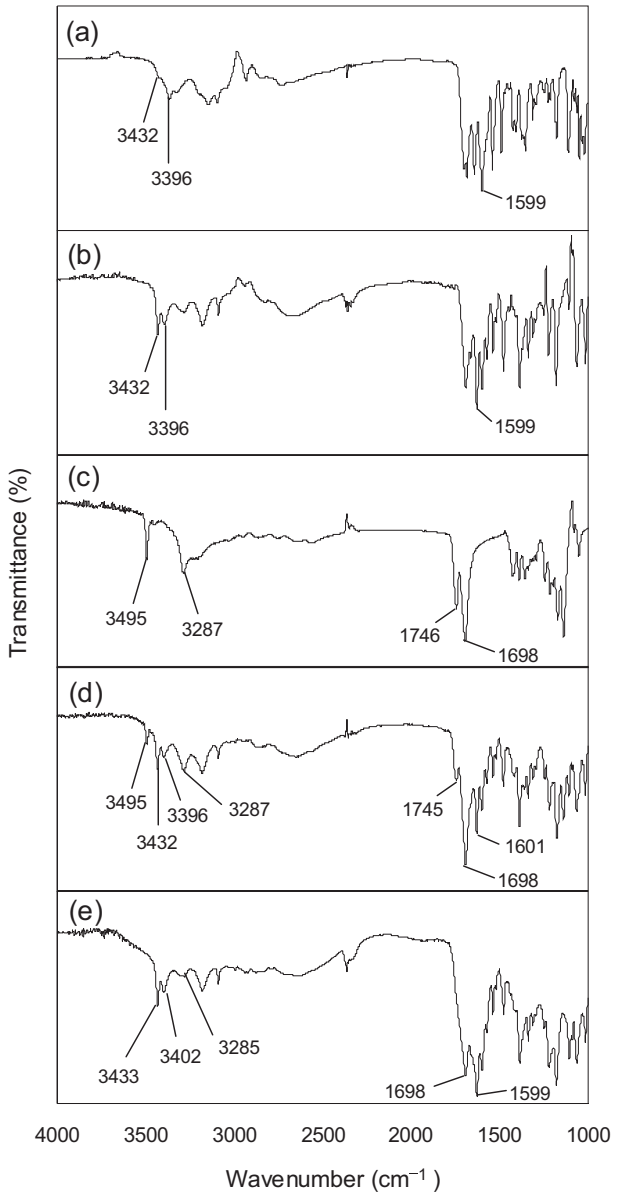

Fig. 5. IR spectra for acyclovir (anhydrous form 1 (a), anhydrous form 2 (b)), citric acid (c), ACV–CA-PM (d), and ACV–CA amorphous (e).

solubility of the cocrystals with that of the anhydrous form and the physical mixture in each solvent. As shown in Fig. 8, the saturated solubility of ACV–TA cocrystals in each solvent was considerably higher than that of acyclovir anhydrous form 2.

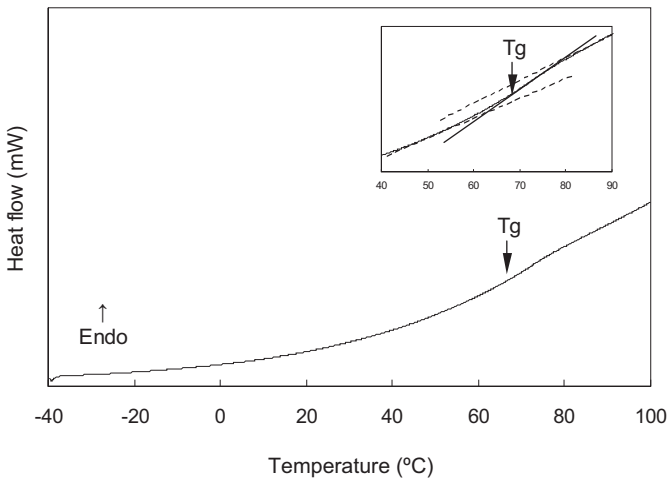

Fig. 6. DSC curve of ACV–CA amorphous.

On the other hand, comparison of the saturated solubility in equilibrium for the cocrystals and the physical mixture at the same drug:excipient proportion showed no remarkable difference. This indicates possibility of some interaction between acyclovir and tartaric acid in each solvent. The saturated solubility of the cocrystals in the solvent was 6.83 ± 0.36 (mg/mL), 5.96 ± 0.01 (mg/mL) and 0.93 ± 0.01 (mg/mL), respectively. In contrast, that of the anhydrous form was 1.09 ± 0.01 (mg/mL), 1.08 ± 0.07 (mg/mL) and 0.13 ± 0.00 (mg/mL), respectively. That of the physical mixture was 6.03 ± 0.61 (mg/mL), 5.46 ± 0.69 (mg/mL) and 0.89 ± 0.07 (mg/mL), respectively.

A dissolution test was conducted to compare the initial dissolution rate of the ACV–TA cocrystals with acyclovir polymorphs and ACV–TA-PM. Fig. 9 shows the initial dissolution profiles for each sample.

The initial dissolution rate of each sample is represented in Table 3.

As shown by the dissolution profiles, the ACV–TA cocrystals dissolved instantaneously, compared with acyclovir polymorphs and ACV–TA-PM. The initial dissolution rate of the cocrystals was three to six times higher than that of acyclovir polymorphs and ACV–TA-PM. The initial dissolution rate of the physical mixture was almost the same as that of acyclovir anhydrous form 2. Although comparison of the saturated solubility in equilibrium for the cocrystals and the physical mixture showed no remarkable difference, that of the initial dissolution rate showed significant difference. This may indicate possibility of the influence of crystal structure change induced by cocrystallization on the initial dissolution rate.

These results indicate that the solubility of acyclovir was improved by cocrystallization.

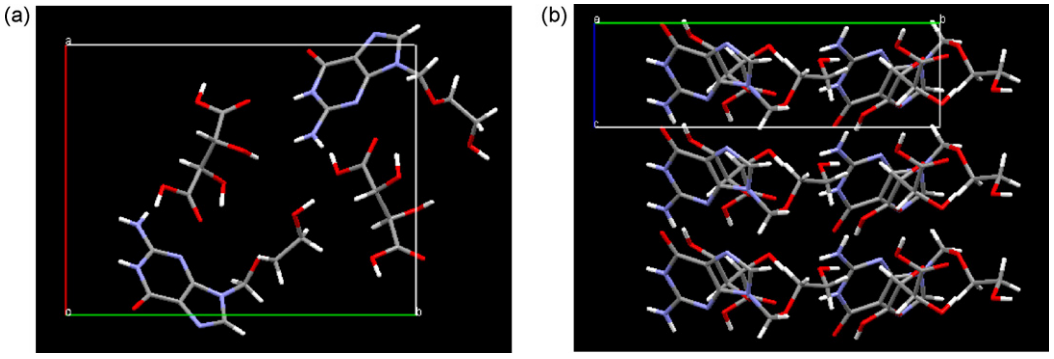

Fig. 7. Packing diagram along the *ab* plane for ACV–TA cocrystal (a) and the *bc* plane for ACV–TA cocrystal (b).

Table 3
Initial dissolution rate of acyclovir polymorph forms and ACV–TA cocrystals in phosphate buffer at 37 °C.

Initial dissolution rate (μg/mL min)					
Anhydrous form 1	Anhydrous form 2	Two-thirds hydrate	Dihydrate	ACV–TA-PM	ACV–TA cocrystal
0.23 ± 0.05	0.14 ± 0.02	0.20 ± 0.07	0.13 ± 0.01	0.13 ± 0.01	0.73 ± 0.13

3.3. Solubility of acyclovir in PEG ointment base

The saturated solubility of ACV–CA amorphous, the crystalline acyclovir and ACV–CA-PM in PEG 400 was determined by HPLC to compare the solubility of the amorphous form in a PEG ointment base with that of the crystalline acyclovir and the physical mixture. As shown in Fig. 10, the saturated solubility of ACV–CA amorphous in PEG 400 at 25 °C was considerably higher than that of the crystalline acyclovir and the physical mixture.

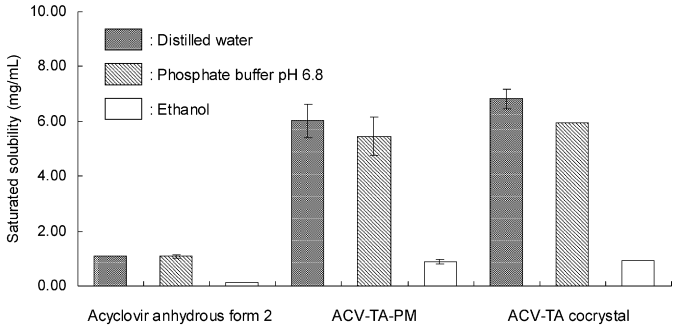

Fig. 8. Saturated solubility of ACV–TA cocrystals, ACV–TA-PM and acyclovir anhydrous form 2 in distilled water, phosphate buffer pH 6.8 and ethanol (*error bars* shows SD, $n = 3$).

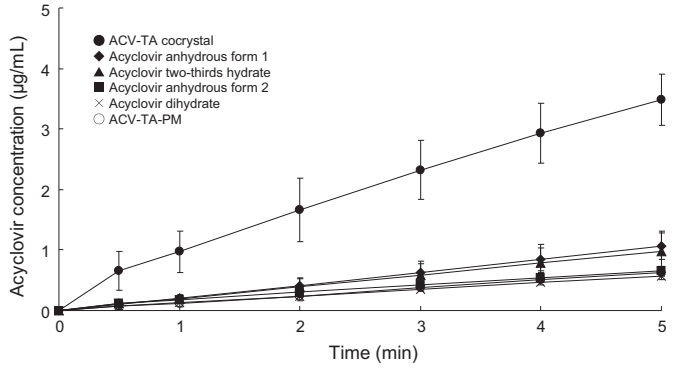

Fig. 9. Dissolution profiles of acyclovir polymorph forms, ACV–TA-PM and ACV–TA cocrystals in phosphate buffer (*error bars* show SD, $n = 3$).

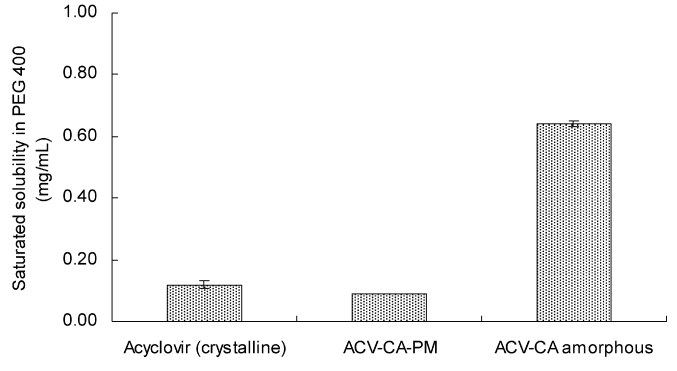

Fig. 10. Saturated solubility of ACV–CA amorphous, ACV–CA-PM and crystalline acyclovir in PEG 400 (*error bars* shows SD, $n = 3$).

The saturated solubility of ACV–CA amorphous, the crystalline acyclovir and the physical mixture was 0.64 ± 0.01 (mg/mL), 0.12 ± 0.01 (mg/mL) and 0.09 ± 0.00 (mg/mL), respectively.

Optical micrographs of PEG ointments containing either 5% acyclovir or ACV–CA-PM or ACV–CA amorphous are shown in Fig. 11.

In PEG ointment containing either 5% acyclovir or ACV–CA-PM, the drug was almost in a crystalline form due to its poor solubility in ointment base. On the other hand, in PEG ointment containing 5% ACV–CA amorphous, the drug was almost dissolved, although it was partially crystallized. This indicates that the drug molecule is present in amounts that exceed the solubility of the drug, as they are dispersed in a PEG ointment base. In this supersaturated system, the thermodynamic activity of the drug seems to rise in temporarily. Therefore, there is a possibility of leading to high skin permeability in PEG ointment containing 5% ACV–CA amorphous.

3.4. In vitro release of acyclovir from PEG ointment

In vitro release profiles of the crystalline acyclovir, ACV–CA-PM and ACV–CA amorphous from PEG ointment are shown in Fig. 12a.

The release profiles show that the drug release rate of ACV–CA amorphous is remarkably higher than that of the crystalline acyclovir and ACV–CA-PM, and the percentage release was almost 100% at 60 min. The drug release rate of the physical mixture was more slightly higher than that of the crystalline acyclovir. This may result from effect of the back-diffusion of release medium into the formulation. The high sensitivity to the back-diffusion may be induced because of the relatively high solubility of citric acid in release medium. The Higuchi equation (Higuchi, 1961) was applied to all data, and the cumulative amount released was plotted vs. the square root of time in Fig. 12b. In ACV–CA amorphous, leveling-off was observed in the profile at later points in time. This phenomenon was thought to be due to the consumption of the solid drug from the ointment base. This suggests that the amorphous solid had already been exhausted later in the experiment because the solubility of the amorphous form was greater than that of the crystalline acyclovir.

3.5. In vitro skin permeation experiments

Fig. 13 shows *in vitro* skin permeation profiles of the crystalline acyclovir, ACV–CA-PM and ACV–CA amorphous, from PEG ointment.

The inset in Fig. 13 shows a close-up of the profile of the crystalline acyclovir and ACV–CA-PM. The profile of ACV–CA amorphous was compared with that of the crystalline acyclovir and ACV–CA-PM. Steady-state permeation was observed from 2 to 26 h, for the amorphous form. The steady-state permeation flux of the amorphous acyclovir was 2.06 μg/cm^2/h. In contrast, the delivery of the crystalline acyclovir (including ACV–CA-PM) from PEG ointment was very slow and steady-state permeation was observed from 22 to 26 h. The flux of the crystalline acyclovir and ACV–CA-PM was 0.02 μg/cm^2/h and 0.09 μg/cm^2/h, respectively. The flux of ACV–CA-PM was more slightly higher than that of the crystalline acyclovir. This indicates possibility of the skin permeation enhancement of the drug by the efficacy of citric acid. The enhancing effect of citric acid on the skin permeation of indapamide has been reported (Ren et al., 2008).

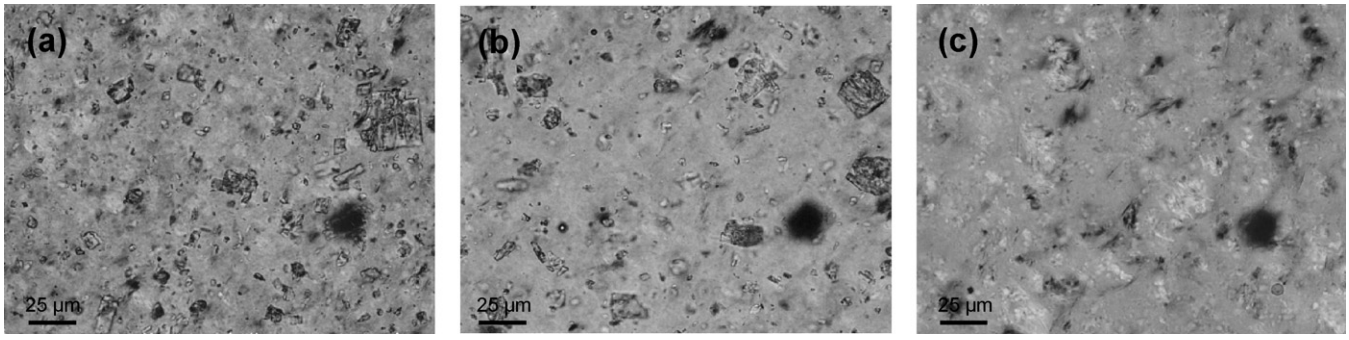

Fig. 11. Optical micrographs of PEG ointments containing either 5% acyclovir (a) or ACV–CA-PM (b) or ACV–CA amorphous (c).

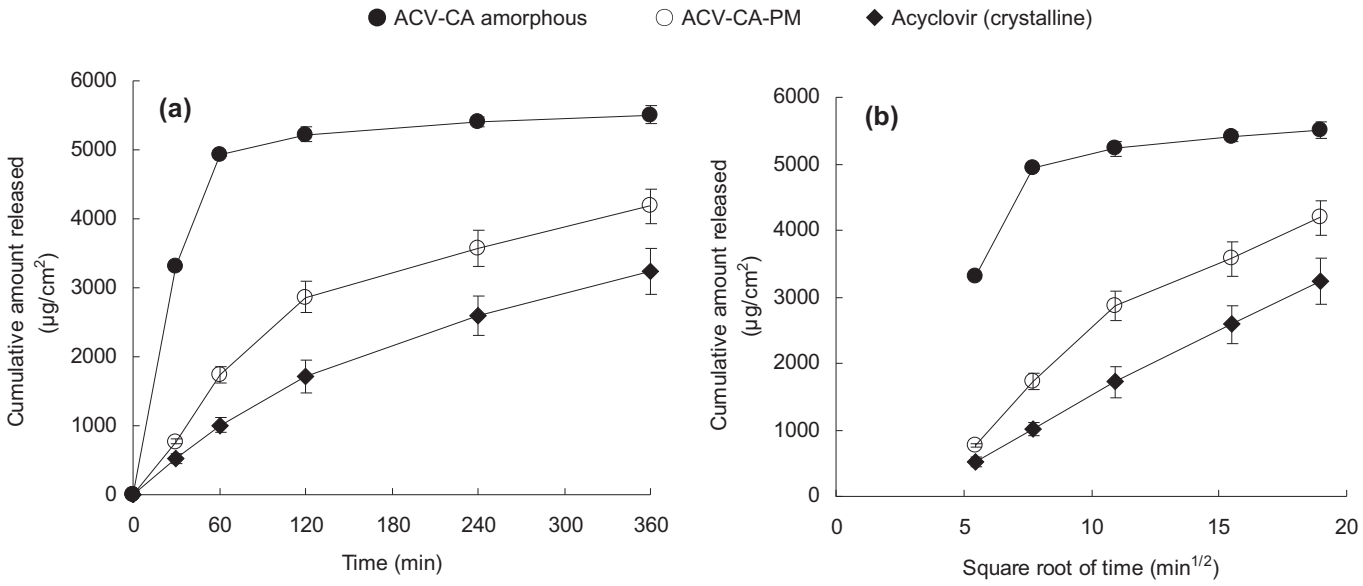

Fig. 12. Released profiles of acyclovir from PEG ointment (a) and Higuchi plots showing rates of release of acyclovir (b).

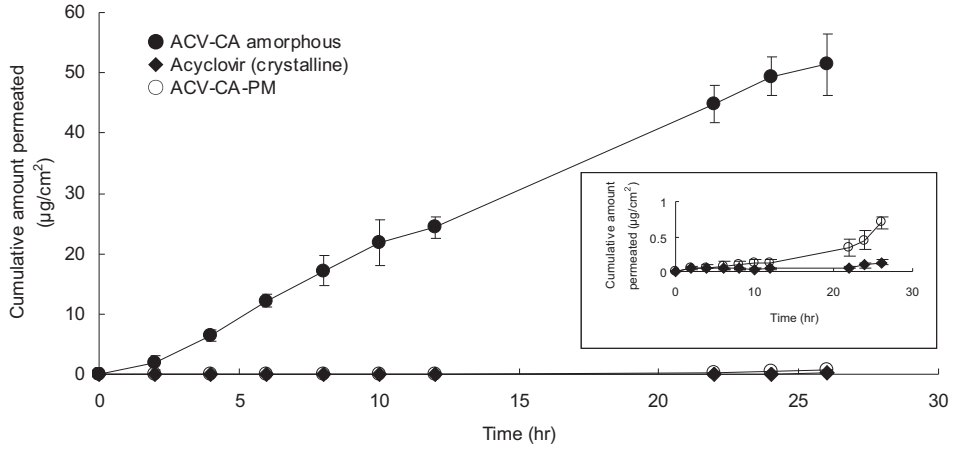

Fig. 13. Permeation profiles of acyclovir through hairless mouse skin from PEG ointment.

The flux was increased remarkably by amorphization of the drug. This correlated well with the results of *in vitro* drug release.

4. Conclusion

In this study, we found novel cocrystals of acyclovir (ACV–TA cocrystals) and characterized the cocrystals using PXRD, TG/DTA, IR, HPLC. The crystal structure of the cocrystal was determined by synchrotron X-ray powder diffraction analysis. To evaluate improvement of the solubility of acyclovir by cocrystallization, the saturated solubility of the cocrystals in distilled water, phosphate buffer pH 6.8 and ethanol was determined and dissolution tests were conducted. In the ACV–TA cocrystal, interaction between acyclovir and tartaric acid mediated by hydrogen bonds was confirmed. The saturated solubility of the cocrystals in each solvents

and the initial dissolution rate of the cocrystals was considerably higher than that of acyclovir.

In addition, we successfully prepared acyclovir amorphous (ACV–CA amorphous) using the interaction between the drug and citric acid. The amorphous form was characterized by PXRD, IR, DSC and HPLC techniques. In the ACV–CA amorphous, interaction between acyclovir and citric acid mediated by hydrogen bonds was confirmed. To evaluate improvement in transdermal absorption of acyclovir effected by amorphization, *in vitro* skin permeation experiments were conducted. It was expected that the amorphous form would be stable at ambient temperature because it has a T_g that is above ambient temperature. The steady-state, *in vitro*, skin permeation flux of the amorphous form was significant higher than that of the crystalline acyclovir.

We successfully improved the pharmaceutically relevant properties of acyclovir, such as the initial dissolution rate and *in vitro* skin permeation, by cocrystallization and amorphization techniques with the use of pharmaceutical excipients.

Acknowledgements

We thank Mr. Hiroyuki Kurobe, Mr. Masataka Ito and Ms. Danyu Li from Toho University for their assistance with the crystal structure analysis.

Synchrotron X-ray powder diffraction experiments were performed under the approval of the Photon Factory Program Advisory Committee (Proposal No. 2010P106).

References

Balfour, H.H., 1999. Drug therapy: antiviral drugs, review. N. Engl. J. Med. 340, 1255–1268.

Barboza, F., Vecchia, D.D., Tagliar, M.P., Silva, M.A.S., Stulzer, H.K., 2009. Differential scanning calorimetry as a screening technique in compatibility studies of acyclovir extended release formulations. Pharm. Chem. J. 43, 363–368.

Benson, H.A.E., 2005. Transdermal drug delivery: penetration enhancement techniques. Curr. Drug Deliv. 2, 23–33.

Berge, S.M., Bighley, L.D., Monkhouse, D.C., 1977. Pharmaceutical salts. J. Pharm. Sci. 66, 1–19.

Brittain, H., 1999. Polymorphism in Pharmaceutical Solids. Marcel Dekker, New York.

Childs, S.L., Hardcastle, K.I., 2007. Cocrystals of piroxicam with carboxylic acids. Cryst. Growth Des. 7, 1291–1304.

Corey, L., Nahmias, A.J., Guinan, M.E., Benedetti, J.K., Critchlow, C.W., Holmes, K.K., 1982. A trial of topical acyclovir in genital herpes simplex virus infections. N. Engl. J. Med. 306, 1313–1319.

Davis, S.S., Hadgraft, J., Al-Kharmis, K., 1981. Percutaneous absorption of methyl salicylate from polyethylene glycol vehicles. J. Pharm. Pharmacol. 33, 97P.

David, W.I.F., Shankland, K., Van de Streek, J., Pidcock, E., Motherwell, W.D.S., Cole, J.C., 2006. DASH: a program for crystal structure determination from powder diffraction data. J. Appl. Crystallogr. 39, 910–915.

Freeman, D.J., Sheth, N.V., Spruance, S.L., 1986. Failure of topical acyclovir in ointmet to penetrate human skin. Antimicrob. Agents Chemother. 29, 730–732.

Friščić, T., Trask, A.V., Jones, W., Motherwell, W.D.S., 2006. Screening for inclusion compounds and systematic construction of three-component solids by liquid-assisted grinding. Angew. Chem. Int. Ed. 45, 7546–7550.

Guy, R.H., Hadgraft, J., 1988. Physicochemical aspects of percutaneous absorption and enhancement. J. Control. Release 5, 753–758.

Hadgraft, J., 1983. Percutaneous absorption: possibilities and problems. Int. J. Pharm. 16, 255–270.

Higuchi, T., 1960. Physical chemical analysis of percutaneous absorption process from creams and ointments. J. Soc. Cosmet. Chem. 11, 85–97.

Higuchi, T., 1961. Rate of release of medicaments from ointment bases containing drugs in suspension. J. Pharm. Sci. 50, 874–875.

Inoue, K., Ogawa, K., Okada, J., Sugibayashi, K., 2005. Enhancement of skin permeation of ketotifen by supersaturation generated by amorphous form of the drug. J. Control. Release 28, 306–318.

Kato, Y., Okamoto, Y., Nagasawa, S., Ueki, T., 1981. Solubility of a new polymorph of phenobarbital obtained by crystallization in the presence of phenytoin. Chem. Pharm. Bull. 29, 3410–3413.

Kaushal, A.M., Gupta, P., Bansal, A.K., 2004. Amorphous drug delivery systems: molecular aspects, design and performance. Crit. Rev. Ther. Drug Carrier Syst. 21, 133–193.

Kirkpatrick, S., Gelatt, C.D., Vecchi, M.P., 1983. Optimization by simulated annealing. Science 220, 671–680.

Kobayashi, N., Saitoh, I., 1998. A method to measure the solubility of drugs in ointment bases. Chem. Pharm. Bull. 46, 1833–1835.

Koizumi, K., Okada, Y., Kubota, Y., Utamura, T., 1987. Inclusion complexes of poorly water-soluble drugs with glucosyl-cyclodextrins. Chem. Pharm. Bull. 35, 3413–3418.

Kozhevina, L.I., Skryabina, L.G., Tselinskii, Yu.K., 1980. The interpretation of the infrared spectrum of tartaric acid. J. Appl. Spectrosc. 33, 1347–1351.

Kristl, A., Srčič, S., Vrečer, F., Šuštar, B., Vojnovic, D., 1996. Polymorphism and pseudopolymorphism: influencing the dissolution properties of the guanine derivative acyclovir. Int. J. Pharm. 139, 231–235.

Larson, A.C., Von Dreele, R.B., 2004. General Structure Analysis System (GSAS). Los Alamos National Laboratory Report LAUR 86-748.

Lu, Q., Zografi, G., 1997. Properties of citric acid at the glass transition. J. Pharm. Sci. 86, 1374–1378.

Luby, J.P., Gnann Jr., J.W., Alexander, W.J., Hatcher, V.A., Friedman-Kien, A.E., Klein, R.J., Keyserling, H., Nahmias, A., Mills, J., Schachter, J., Douglas, J.M., Corey, L., Sacks, S.L., 1984. A collaborative study of patient-initiated treatment of recurrent genital herpes with topical acyclovir or placebo. J. Infect. Dis. 150, 1–6.

Luengo, J., Arángiuz, T., Sepúlveda, J., Hemández, L., Plessing, C.V., 2002. Preliminary pharmacokinetics study of different preparations of acyclovir with β-cyclodextrin. J. Pharm. Sci. 91, 2593–2598.

Lutker, K.M., Quiñones, R., Xu, J., Ramamoorthy, A., Matzder, A.J., 2011. Polymorphs and hydrates of acyclovir. J. Pharm. Sci. 100, 949–963.

Patel, D., Sawant, K.K., 2007. Oral bioavailability enhancement of acyclovir by self-microemulsifying drug delivery system (SMEDDS). Drug Dev. Ind. Pharm. 33, 1318–1326.

Pawley, G.S., 1981. Unit-cell refinement from powder diffraction scans. J. Appl. Crystallogr. 14, 357–361.

Rao, M.K., Narayanaswamy, C.K., 1970. Infrared spectrum of anhydrous citric acid in the solid state. Indian J. Phys. 44, 34–38.

Reichman, R.C., Badger, G.J., Guitan, M.E., Nahmias, A.J., Keeney, R.E., Davis, L.G., Ashikaga, T., Dolin, R., 1983. Topically administered acyclovir in the treatment of recurrent herpes simplex genitalis: a controlled trial. J. Infect. Dis. 147, 336–340.

Ren, C., Fang, L., Li, T., Wang, M., Zhao, L., He, A., 2008. Effects of permeation enhancers and organic acids on the skin permeation of indapamine. Int. J. Pharm. 350, 43–47.

Rossel, C.P., Carreño, J.S., Baeza, M.R., Alderete, J.B., 2000. Inclusion complex of the antiviral drug acyclovir with cyclodextrin in aqueous solution and in solid phase. Quim. Nova 23, 749–752.

Sachan, N.K., Pushkar, S., Solanki, S.S., Bhatere, D.S., 2010. Enhancement of solubility of acyclovir by solid dispersion and inclusion complexation methods. World Appl. Sci. J. 11, 857–864.

Serajuddin, A.T.M., 1999. Solid dispersion of poorly water-soluble drugs: early promises, subsequent problems, and recent breakthroughs. J. Pharm. Sci. 88, 1058–1066.

Sohn, Y.T., Kim, A.H., 2008. Polymorphism and pseudopolymorphism of acyclovir. Arch. Pharm. Res. 31, 231–234.

Spruance, S.L., Crumpacker, C.S., Schnipper, L.E., Kern, E.R., Marlowe, S., Arndt, K.A., Overall Jr., J.C., 1984. Early, patient-initiated treatment of herpes labialis with topical 10% acyclovir. Antimicrob. Agents Chemother. 25, 553–555.

Spruance, S.L., Schnipper, L.E., Overall Jr., J.C., Kern, E.R., Arndt, E.R., Chiu, G.L., Crumpacker, C.S., 1982. Treatment of herpes simplex labialis with topical acyclovir in polyethylene glycol. J. Infect. Dis. 146, 85–90.

Squillante, E., Needham, T., Zia, H., 1997. Solubility and in vitro transdermal permeation of nifedipine. Int. J. Pharm. 15, 171–180.

Stahl, P.H., Wermuth, C.G., 2002. Handbook of Pharmaceutical Salts. Wiley-VCH, Weinheim.

Stott, P.W., 1998. Transdermal delivery from eutectic systems: enhanced permeation of a model drug, ibuprofen. J. Control. Release 50, 297–308.

Szeman, J., Ueda, H., Szejtli, J., Fenyvesi, E., Machida, Y., Nagai, T., 1987. Enhanced percutaneous absorption of homogenized tolnaftate/beta-cyclodextrin polymer ground mixture. Drug Des. Deliv. 1, 325–332.

Whitley, J.R., Whelchel, J., Diethelm, A.G., Kartus, P., Soong, S.-J., 1984. Infections caused by herpes simplex virus in the immunocompromised host: natural history and topical acyclovir therapy. J. Infect. Dis. 150, 323–329.